Chapter 2
Recent Changes in Arctic Vegetation: Satellite Observations and Simulation Model Predictions

**Scott J. Goetz, Howard E. Epstein, Uma S. Bhatt, Gensuo J. Jia,
Jed O. Kaplan, Heike Lischke, Qin Yu, Andrew Bunn, Andrea H. Lloyd,
Domingo Alcaraz-Segura, Pieter S.A. Beck, Josefino C. Comiso,
Martha K. Raynolds, and Donald A. Walker**

Abstract This chapter provides an overview of observed changes in vegetation productivity in Arctic tundra and boreal forest ecosystems over the past 3 decades, based on satellite remote sensing and other observational records, and relates these to climate variables and sea ice conditions. The emerging patterns and relationships are often complex but clearly reveal a contrast in the response of the tundra and boreal biomes to recent climate change, with the tundra showing increases and undisturbed boreal forests mostly reductions in productivity. The possible reasons for this divergence are discussed and the consequences of continued climate warming for the vegetation in the Arctic region assessed using ecosystem models, both at the biome-scale and at high spatial resolution focussing on plant functional types in the tundra and the tundra-forest ecotones.

2.1 Introduction

Ecosystem responses to warming of the Arctic have the potential to feed back either positively or negatively to the climate system depending on changes in the disturbance regime, vegetation distribution and productivity (McGuire et al. 2009). The lower albedo of forest vegetation compared with tundra, for example, results in a positive feedback on temperature (Bala et al. 2007; Chapin et al. 2005; Randerson et al. 2006). Conversely, increased productivity of arctic vegetation resulting from warmer temperatures tends to result in increased carbon dioxide (CO_2) uptake by net photosynthesis, providing a negative feedback to rising temperatures (Field et al. 2007; Serreze et al. 2000). Drought can modify this feedback effect, decoupling warming and productivity, as can the balance of gross photosynthesis and plant respiration, which varies substantially by plant functional type (Chapin et al. 1996; Goetz and Prince 1999). The relative importance of these competing feedbacks, and thus the cumulative effect of changing arctic vegetation on the climate system, is still not well known. For boreal forest ecosystem (and possibly tundra as well) this

S.J. Goetz (✉)
The Woods Hole Research Center, 149 Woods Hole Road, Falmouth, MA 02540-1644, USA
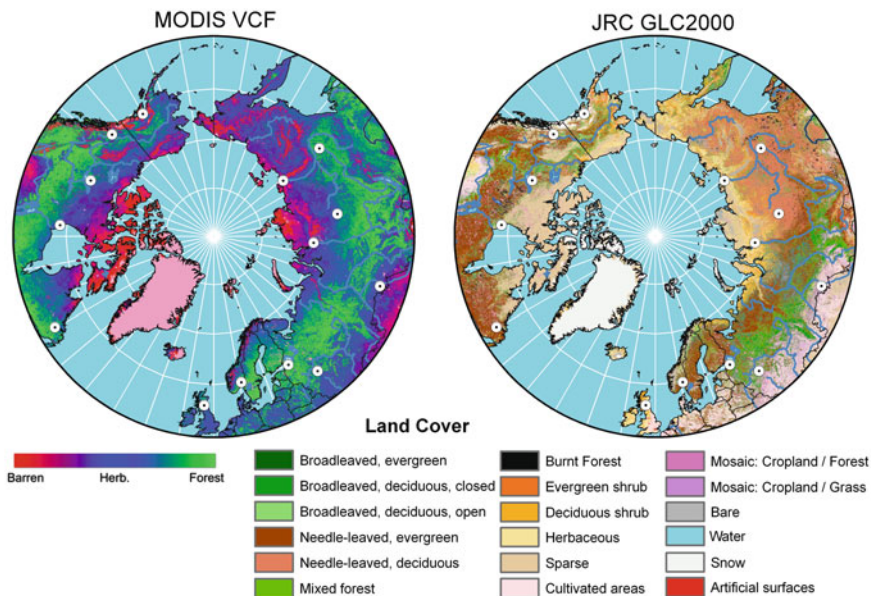e-mail: sgoetz@whrc.org

Fig. 2.1 (*left*) A color composite of the MODIS vegetation continuous fields indicating a combination of tree and herbaceous vegetation cover and bare ground. As the *circular legend* indicates, *green hues* indicate dominance of tree cover, *blue hues* indicate dominance of herbaceous vegetation (tundra), and *red hues* indicate bare ground. (*right*) A Global Land Cover 2000 map of vegetation cover types, as indicated in the legend. The *white dots* indicate major towns and are useful for referencing between the two images. Adapted from Bunn and Goetz (2006)

depends substantially upon the frequency and severity of the fire disturbance regime (Achard et al. 2008; Goetz et al. 2007; Kasischke and Stocks 2000; Mack et al. 2008; Randerson et al. 2006; Soja et al. 2007).

In this chapter, we focus primarily on changes in the productivity of arctic ecosystems in recent decades (<30 years), specifically tundra and boreal forest, as observed with a combination of satellite observations (Fig. 2.1) and field measurements, as projected by simulation modeling. We first provide an overview of changes documented in the recent literature, including our own work, and then focus on a series of case studies emphasizing more recent documented changes within Northern Eurasia. We end with a series of modeling studies that explore the likely future responses of vegetation to climate warming, focusing separately on tundra and boreal forest ecosystems.

2.2 An Overview of Recent Changes in Arctic Vegetation Productivity

Analyses of productivity metrics derived from satellite observations at high latitudes indicate that past evidence for ubiquitous "greening" trends that had been
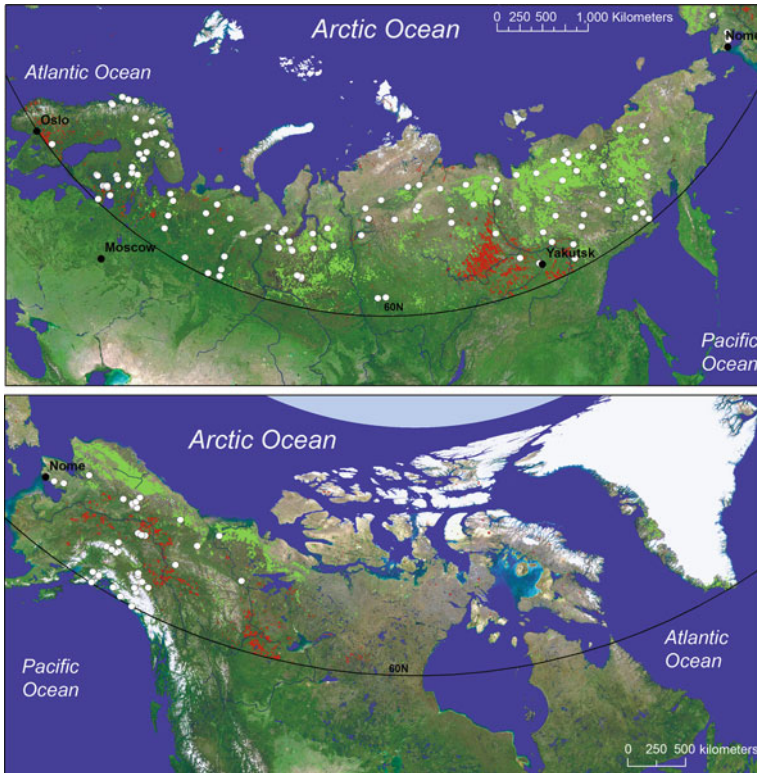
Fig. 2.2 Trends in satellite observations of vegetation productivity derived from a 1982 to 2005 time series of GIMMS-GAVHRR vegetation indices at 8-km spatial resolution, with significant positive trends shown in *bright green* and negative trends in red. Tree ring measurement sites are indicated as *white dots*. The trends map is overlaid on a 1-km resolution natural color composite of MODIS imagery. *White colors* in the MODIS image represent snow and ice. Compare these trends with tree cover and land cover maps in Fig. 2.1

widely noted (Jia et al. 2003; Myneni et al. 1997; Nemani et al. 2003; Slayback et al. 2003) did not continue after ~1990. The observed changes post-1990 were non-uniform across the broad Arctic domain, particularly after 2000 (Bunn and Goetz 2006; Goetz et al. 2005; Jia et al. 2006; Neigh et al. 2008). Arctic tundra vegetation increased both in terms of peak productivity and growing season length between 1982 and 2005 (see Fig. 2.2), and this finding is supported by a wide range of field site measurements across Northern Eurasia and the high latitudes of North America (ACIA 2004; Serreze et al. 2000; Walker et al. 2006). These dynamics include changes in the composition and density of herbaceous vegetation (Epstein et al. 2004; Shaver et al. 2007), increased woody shrub encroachment in tundra areas (Sturm et al. 2001; Tape et al. 2006), greater depths of seasonal thaw (Goulden et al. 1998; Kimball et al. 2006; Schuur et al. 2009), and associated changes in the energy regime (Chapin et al. 2005; Sturm et al. 2001).

In forested areas, by contrast, few areas not recently disturbed by fire showed any significant positive trend in productivity over the same time period, with the

exception of the West Siberian lowlands and areas with a low density of larch forest in the far east of Russia (Fig. 2.1). In North America more than 25% of undisturbed forest areas actually experienced a decline in productivity (Goetz et al. 2005). These same areas showed no systematic change in growing season length. Climatic warming occurred across the entire Arctic, but the forest response indicates that neither the intensity nor the length of the growing season changed in a way that reflected a simple relationship with increasing temperature or CO_2. The productivity trends in forested areas were most evident in the latter part of the growing season, indicating impacts of late summer drought (Vapor Pressure Deficit, VPD) on stomatal control and photosynthesis (Bunn et al. 2007; Zhang et al. 2008). Related, more densely forested areas were significantly more likely to show strong negative productivity trends (Bunn and Goetz 2006), particularly areas along the Lena River, west of Yakutsk in Siberia, and in black spruce forests of interior Alaska and central Canada (Goetz et al. 2007). These observations are supported by other recent modeling work comparing anomalies in simulated net productivity to gridded climate data, indicating that net photosynthetic gains being made in the spring months are more than offset by net photosynthetic losses later in the summer (Angert et al. 2005; Zhang et al. 2008). As noted above, these trends in productivity across unburned areas are heavily dependent on cover type and the underlying vegetation density (see Figs. 2.1 and 2.2).

2.3 Tundra Ecosystems

2.3.1 Relationships Among Sea Ice, Land Surface Temperature and Productivity

Recent dramatic reductions in summer sea-ice, particularly perennial ice, have been documented in the Arctic (Comiso 2002; Stroeve et al. 2006) and are of growing concern. Reduced sea-ice may exacerbate surface air warming, leading to increased permafrost thawing and vegetation productivity, and also potentially modifying the habitat and migration characteristics of both marine and terrestrial fauna. Our analysis documents some of these changes using ice cover derived from historical passive microwave data, surface temperature data from historical thermal infrared data, and vegetation indices (i.e. the normalized difference vegetation index [NDVI]) as a metric of vegetation productivity.

To investigate the nature of these connections, we examined the relationship between coastal ice and the adjacent land surface. The analysis employs 25-km resolution Special Sensor Microwave Imager (SSMI) estimates of sea ice concentration, based on a bootstrap algorithm (Comiso 2008), and AVHRR radiometric surface temperature (Comiso 2003, 2006), both covering the 26-year period from January 1982 to December 2007. The surface temperature data have recently been enhanced by applying more effective cloud masking techniques and an improved consistency in calibration through the utilization of in situ surface temperature data. The NASA

GIMMS NDVI data were used for the 1982–2007 summer periods. The Maximum NDVI (MaxNDVI) is the highest NDVI value obtained during the summer for each 8-km pixel and represents the peak greenness achieved during the summer. The Time-Integrated NDVI (TI-NDVI) is the sum of the biweekly NDVI values for the summer growing season. A threshold of 0.09 was used as a minimal value for green vegetation, based on an analysis of spring green-up (Jia et al. 2004). The NDVI data sets were resampled to 25-km resolution for comparisons with climate and sea-ice data sets. The NDVI analysis was limited to the area south of 72°N because of a discontinuity in the GIMMS data north of this latitude.

The spatial variations of the climate-vegetation relationships were examined for Eurasia regionally using the divisions of Treshnikov (1985) (Fig. 2.3) and for the total Eurasian domain. NDVI and summer warmth index (SWI – sum of mean monthly temperatures >0°C) time series were constructed for the tundra between treeline and 72°N (the position of the discontinuity in the NDVI data). The area south of 72° includes nearly all the Low Arctic that has more or less continuous cover of plants and peaty soil surface horizons (Walker 2005). Sea-ice indices were constructed over a corresponding 50-km ocean zone for each region. The sea-ice concentration is an average each year of the 3 weeks centered on the week of 50% climatological ice concentration, which varies by region and falls between 15 May and 22 July for the Eurasian study regions. This period was selected as it describes the transition to summer for most of the Arctic regions in our study. For correlation analyses, sea-ice concentrations were compared with SWI for 50-km seaward and landward strips along the entire Arctic coastline. For the correlations with NDVI, only the sea-ice concentrations and SWI south of 72°N were used.

The regional year-to-year variability and trends in SWI, sea-ice concentration and NDVI indices are relatively large (Fig. 2.3a–g), but there are consistent positive trends for SWI and TI-NDVI and negative trends for sea-ice concentration, albeit of varying strength, among the regions. The largest decreases in coastal sea-ice occurred in the E. Siberia and W. Chukchi seas (−49 and −47%). The largest change in summer land temperature occurred in the W. Chukchi, W. Bering, and E. Siberia Seas (+68%, +39%, +35%). More modest changes in SWI occurred elsewhere, varying from +2% in the Laptev Sea to 14% in the Barents Sea. The trends in TI-NDVI ranged from +5% in the Barents Sea to +15% in the W. Bering Sea. MaxNDVI changes varied from −1% in the Barents and W. Chukchi seas to +9% in the Laptev and W. Bering seas. For the Eurasian Arctic coast as a whole sea-ice has decreased (−29%), and SWI has increased (+16%) (Fig. 2.4a). MaxNDVI increased 4% and the TI-NDVI increased 8% (Fig. 2.4b).

The correlations between sea-ice concentration, SWI and TI-NDVI for each region are generally strong in all seas (Table 2.1), indicating that yearly variations in sea ice correspond to variations in land-surface temperatures and TI-NDVI. The exception in the West Bering region where spring sea ice and TI-NDVI are not correlated may be due to the importance of other processes, such as strong controls of NDVI by terrain and substrate variables (Raynolds 2009). For the entire Eurasia domain, sea-ice concentration and SWI were negatively correlated ($r = -0.57$, $p < 0.05$). TI-NDVI was significantly correlated with SWI ($r = 0.57$, $p < 0.05$) and
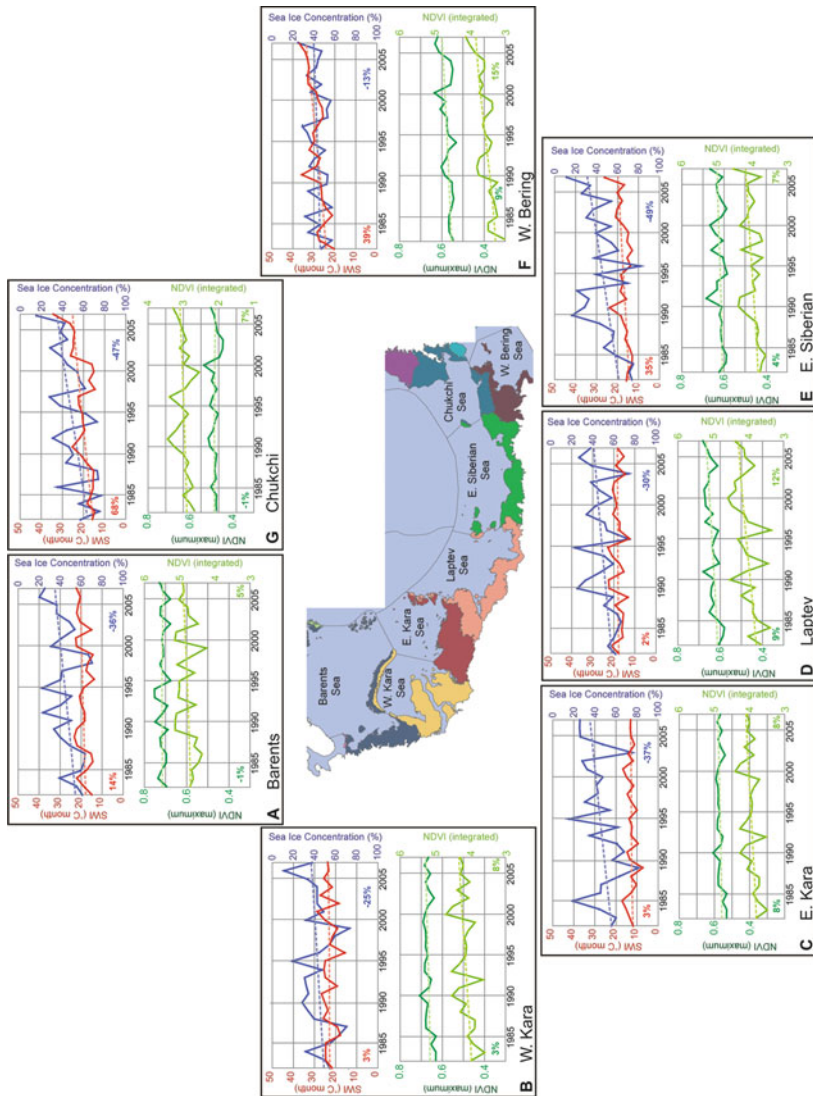
Fig. 2.3 Northern Eurasia regional (region defined by color) time series of sea-ice concentration (*blue*), and TI-NDVI (*light green*), and TI-NDVI (*light green*). Sea-ice concentrations and SWI are for 50-km zones along the land and ocean. NDVI is for the tundra region south of 72°N. Decadal trends are indicated by color-coded numbers, with color corresponding to the line variable and bolded trends are significant at *p* < 0.05. All lines cover 1982–2007. Note the limits but not the scale on the TI-NDVI axis are different for the W. Chukchi. Based on Bhatt et al. (2008)
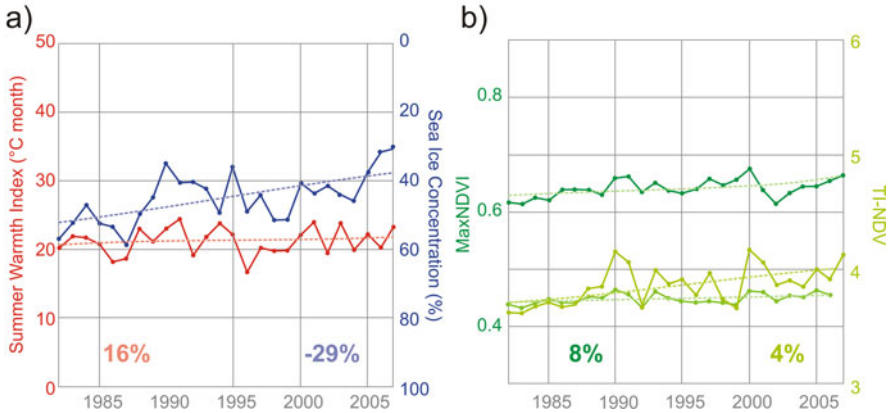
Fig. 2.4 (**a**) Northern Eurasia time series of Summer Warmth Index (*red*), 4–22 June sea-ice concentration (*blue*) in 50-km zones along the land and ocean. Note that sea ice concentration has a reversed scale. (**b**) Maximum NDVI (*dark green*) and integrated NDVI (*light green*) for the tundra region south of 72°N. Decadal trends are indicated by color coded numbers, with color corresponding to the line variable and bolded trends are significant at $p < 0.05$. All lines cover 1982–2007. Based on Bhatt et al. (2008)

Table 2.1 Correlations between SWI, sea-ice concentration, and TI-NDVI for subregions of coastal Eurasia. The sea-ice concentrations were correlated with SWI for 50-km seaward and landward strips along the entire Arctic coastline. For the correlations with TI-NDVI, only the sea-ice concentrations and SWI south of 72°N were used

Region	SWI – Sea ice	SWI – TI-NDVI	Sea-ice – TI-NDVI
Barents	−0.55*	0.60*	−0.49*
Kara-Yamal	−0.41*	0.59*	−0.31
Kara-East	−0.41*	0.62*	N/A
Laptev	−0.71*	0.74*	−0.68*
E. Siberian	−0.64*	0.49*	−0.72*
Chukchi	−0.52*	0.59*	−0.49*
W. Bering	0.0	0.54*	0

An asterisk (∗) indicates significance at the 95% level or greater. Correlations are based on linearly detrended time series. Real forest change: preditio

sea-ice concentration ($r = -0.54$, $p < 0.05$), indicating that enhanced greenness of tundra vegetation occurs with a warmer growing season and reduced sea-ice. Yearly variations in MaxNDVI, however, were not significantly correlated with sea-ice or SWI.

To examine the relationships between the large-scale climate drivers and Arctic sea-ice, SWI and NDVI, co-variability and correlations with climate indices were conducted. The climate indices used for this study include the December–March values for the North Atlantic Oscillation (NAO), Northern Annular Model (NAM or Arctic Oscillation), Pacific Decadal Oscillation (PDO) and North Pacific Index (NPI). The NAO is a measure of the north-south surface pressure gradient in

the North Atlantic, whereas the NAM is more of a hemispheric measure of this pressure gradient. The PDO describes sea-surface temperature (SST) in the North Pacific (a positive PDO index indicates cool water), and the NPI is a measure of the Aleutian Low pressure system in the North Pacific (negative index values indicate anomalously low sea level pressure). The NAO, NAM and NPI indices were provided by the National Center for Atmospheric Research (NCAR, www.cgd.ucar.edu/cas/jhurrell/). The PDO was provided by the Joint Institute for the Study of the Atmosphere and Ocean (JISAO, jisao.washington.edu/pdo/).

Relationships between Eurasian SWI, sea-ice, and TI-NDVI and climate indices are shown in Table 2.2. None of the climate indices were significantly correlated with land temperatures (SWI). The NAO, and NAM indices were significantly negatively correlated with sea-ice concentration ($r = -0.44$ and -0.53, respectively). The PDO was negatively correlated with TI-NDVI ($r = -0.50$), and the NPI and NAO were significantly positively correlated with TI-NDVI ($r = 0.44$ and 0.39, respectively). The positive phase of the NAO and NAM is generally characterized by enhanced storminess in the Arctic, increased heat transport from lower latitudes, and warmer winter temperatures. The positive phase in the NAO/NAM is consistent with decreased sea-ice, increased SWI and enhanced greenness. The negative correlation between PDO and TI-NDVI is intriguing because the interactions between the Northern Eurasia land mass and the PDO are currently not well understood (Pavelsky and Smith 2004). The significant correlations with the NPI were opposite those for the PDO (which is consistent with the inverse correlation of the NPI and PDO). Essentially the PDO increases while SWI and NDVI decrease, whereas the NPI has the opposite correlations.

This analysis indicates that there is coherent variability of SWI, sea-ice concentrations and vegetation productivity in adjacent land–ocean regions of the coastal Eurasian Arctic, where decreased sea ice is found with increased summer warmth and increased tundra productivity. This relationship holds at the continental scale and also regionally in Eurasia. There are significant correlations of sea-ice concentration, SWI and integrated NDVI with the previous winter (December–March) climate indices. This is consistent with the growth of sea-ice area during winter months and relative melting during the following spring and summer (e.g. Deser et al. 2000). While this analysis is consistent with the hypothesis that sea-ice changes are forcing vegetation changes, it is not conclusive because correlations

Table 2.2 Correlations among SWI, sea-ice concentration, and integrated NDVI in 50-km zones within subregions of coastal Eurasia

Region	SWI	Sea-ice	TI-NDVI
NAO	0.36	−0.44*	0.31
NAM	0.17	−0.53*	0.39*
PDO	−0.15	0.38	−0.50*
NPI	0.24	−0.26	0.44*

An asterisk (∗) indicates significance at the 90% level or greater

only establish co-variability and not causality. Further work is necessary to understand these relationships.

2.3.2 Variability of Tundra Productivity Within Bioclimatic Subzones: Focus on the Yamal Peninsula

We focused a more detailed examination of Eurasian tundra vegetation dynamics on the Yamal Peninsula, a region of northwestern Siberia that includes a relatively uninterrupted latitudinal gradient. Our analysis of inter-annual trends in tundra vegetation using satellite data encompassed all five of the arctic bioclimate subzones (Walker et al. 2005). Three of the five subzones (C–E) exist on mainland Yamal, while the other two are on islands in the Kara Sea. We combined remote-sensing, time-series data with multi-scale analyses for identifying areas of relatively pure vegetation to investigate recent changes in vegetation greenness along the latitudinal temperature and vegetation gradient of the Yamal tundra.

We again used the NASA GIMMS time series at 8-km resolution and bimonthly temporal resolution, and also included a land-cover type product derived from Moderate-Resolution Imaging Spectroradiometer (MODIS) imagery (Friedl et al. 2002) for finer scale discrimination of vegetation cover. The temporal analysis was performed with the 1982–2005 time series, stratified by bioclimate subzone. We examined changes of vegetation greenness over the 24 year record, as indicated by variations of the annual maximum NDVI, spanning High Arctic (Subzones A–C) and Low Arctic (Subzones D and E) ecosystems. Subpixel fractional vegetation cover was used to select homogenously vegetated areas of tundra throughout the Yamal region. Autoregression analysis to account for temporal autocorrelation in the data set was performed on the NDVI time series of selected, relatively homogenous areas for each subzone. Image data quality north of 70° latitude for 2004–2005 was poor due at least in part to calibration issues with AVHRR data, so only areas south of 70°N were analyzed for those years.

Linear regressions in arctic tundra vegetation greenness over the analysis period were significantly positive ($\alpha < 0.05$) for each Yamal subzone, with 82.7% of the analyzed pixels showing positive trends throughout the period 1982–2003. The average rate of change in maximum NDVI was +0.44% year^{-1} for the entire arctic Yamal ($r^2 = 0.61$, $p < 0.001$). For south of 70°N from 1982 to 2005, the average rate of change was +0.34% year^{-1} (Fig. 2.5). Vegetation productivity was expected to increase from north to south along this bioclimatic gradient; therefore, NDVI was greater in areas below 70°N relative to the full regional extent.

Changes were heterogeneous among subzones. Annual peak values of NDVI increased by 0.41–0.56% year^{-1} over the High Arctic (Subzones A–C) where prostrate dwarf shrubs, forbs, mosses and lichens dominate, and by 0.28–0.37% year^{-1} over the Low Arctic (Subzones D and E) where erect shrubs and graminoids dominate (Fig. 2.6). There was similar inter-annual variation (i.e., years of high NDVI and years of low NDVI) among the five subzones, despite the differences in NDVI
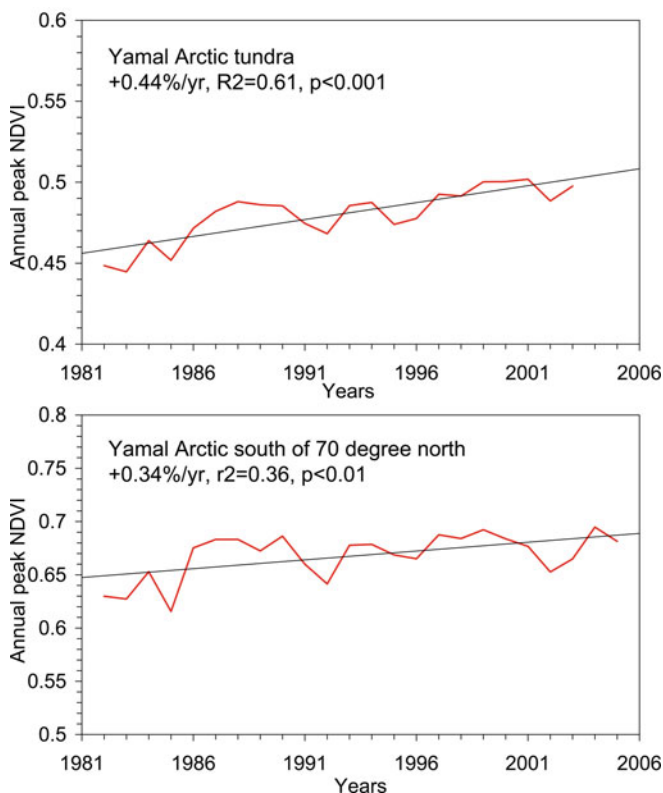
Fig. 2.5 (*top*) Changes in annual peak vegetation greenness (NDVI) over the entire Yamal region from 1982 to 2003 and (*bottom*) below 70°N from 1982 to 2005 as detected by NOAA AVHRR time series data. Annual peak NDVI represents the maximum NDVI values for each year. *Black lines* represent linear regressions. Data quality is low beyond 70°N for 2004–2005 due to calibration errors. The greening trends for the data set are +0.44% year^{-1} ($r^2 = 0.61$, $p < 0.001$) for the entire region from 1982 to 2003 and +0.34% year^{-1} ($r^2 = 0.36$, $p < 0.01$) south of 70°N from 1982 to 2005

magnitudes. Peak vegetation greenness was relatively low in the early 1980s and increased slowly over that decade. A sharp decline of greenness was observed in 1992, which is largely related to the Mt. Pinatubo eruption in late 1991. Following that decline, the trend of greening continued a gradual ascent.

The greatest rates of greening were observed for bioclimate Subzones A and B, in the northern High Arctic and polar desert (a classification specific to Subzone A). These subzones cover parts of Ostrov Belyy and Novaya Zemlya, islands located north and northwest of the Yamal Peninsula, respectively. Subzone A had the highest rate of increase of peak vegetation greenness (0.56% year^{-1}), closely followed by Subzone B (0.54% year^{-1}). Subzones A and B have very short growing seasons and low vegetation cover. Subzone A is characterized by the absence of any
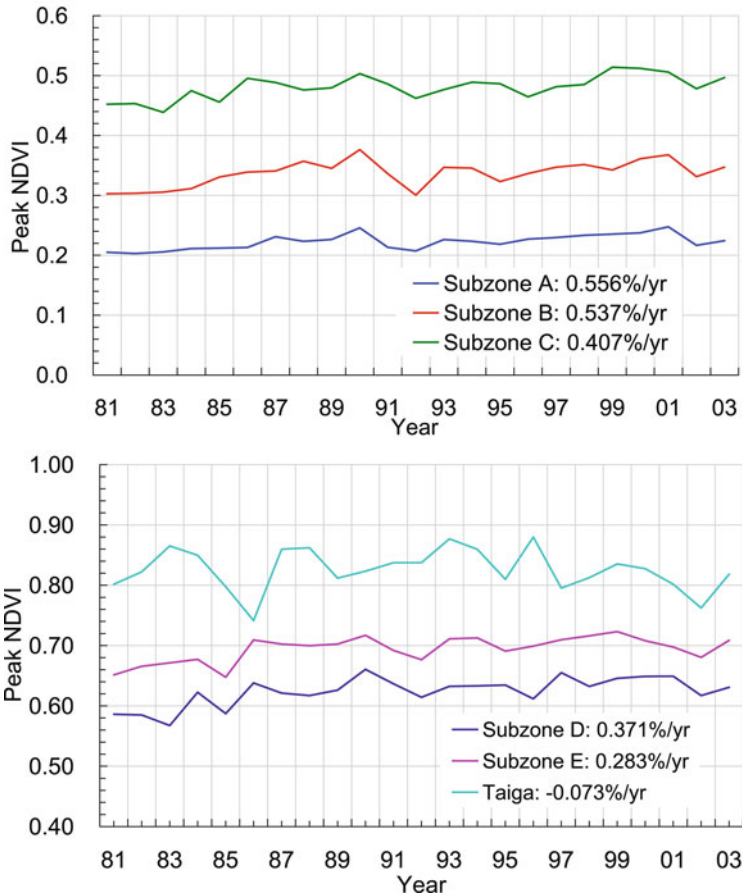
Fig. 2.6 Changes of annual peak vegetation greenness (NDVI) over each of the five arctic tundra bioclimate subzones of the Yamal, in addition to the northern taiga from 1982 to 2003 as detected by NOAA AVHRR time series data

woody plants, whereas Subzone B contains a few species of prostrate dwarf shrubs. Due to the short growing season and sparse vegetation, we were surprised to find a strong increase in peak greenness in this area. Factors that may have contributed to the greening are an increase in plant height and coverage due to warming, and possibly a more rapid earlier growth of tundra plants, as indicated by an earlier date of peak greenness (Jia et al. 2004). Mosses and lichens are persistent in these harsh environments and may respond to environmental changes more rapidly than vascular plants, enhancing their photosynthesis even during very short, favorable periods.

The lowest rate of peak greenness change was observed in Subzone E, dominated by dwarf-erect and low deciduous shrubs such as birch (e.g., *Betula nana*),

willow (*Salix spp.*) and alder (*Alnus crispa*), followed by Subzone D that is covered by sedges and erect dwarf shrubs. Located at the southern boundary of the arctic tundra biome, Subzone E has experienced an enhancement of shrub cover and the slow colonization of tree species, potentially triggered by increased surface temperatures and a deeper snow pack, which insulates the soil and increases nutrient mineralization (e.g., Shaver and Chapin 1991). Increases in fractional cover of shrubs and small trees would lead to higher NDVI values, as recently documented by Forbes et al. (2010). However, anthropogenic disturbances can be intense for mainland Yamal (Subzones C–E relative to Subzones A–B), as the arctic tundra of mainland Yamal has long been used by the Nenets people for reindeer herding. Over the past 2 decades both the Nenets population and reindeer numbers have increased substantially, putting greater pressure on the vegetation. Meanwhile, oil and natural gas exploration and extraction have increased in the region over the same time period, as new and larger fields were discovered in the 1980s and 1990s (see Forbes et al. 2009). Reindeer grazing can produce large areas of reduced vegetation, while construction of drilling platforms and service roads have created dense vehicle tracks and bare scars that are clearly detectable from higher resolution satellite data. The effects of these disturbances may have reduced the propensity for greater vegetation growth in Subzones D and E.

2.4 Boreal Forest Ecosystems

In addition to the changes documented in tundra vegetation, there have been several recent advances in understanding boreal tree responses to changing climate in the Arctic. The recent declines in productivity of many boreal forest areas, aside from recently disturbed areas, suggest that warming may not produce a negative feedback to additional warming (i.e., increased CO_2 sequestration), as had widely been expected. Moreover some positive feedbacks may result from advances of latitudinal tree-line, as has been widely documented in areas experiencing increased temperatures (e.g., Lloyd 2005), and these changes would also alter energy feedbacks associated with albedo changes. The responses of different tree species to warming vary substantially, however, as documented in the next section.

2.4.1 Tree Rings as an Integrative Measure of Growth

There are hundreds of publicly available tree growth data sets from tree rings for the northern high latitudes that are archived in the International Tree-Ring Data Bank, maintained by the National Oceanic and Atmospheric Administration's World Data Center for Paleoclimatology (http://www.ncdc.noaa.gov/paleo). A recent study by Lloyd and Bunn (2007) examined the associations between gridded climate data and tree growth for 232 sites across the northern high latitudes (see Fig. 2.1).
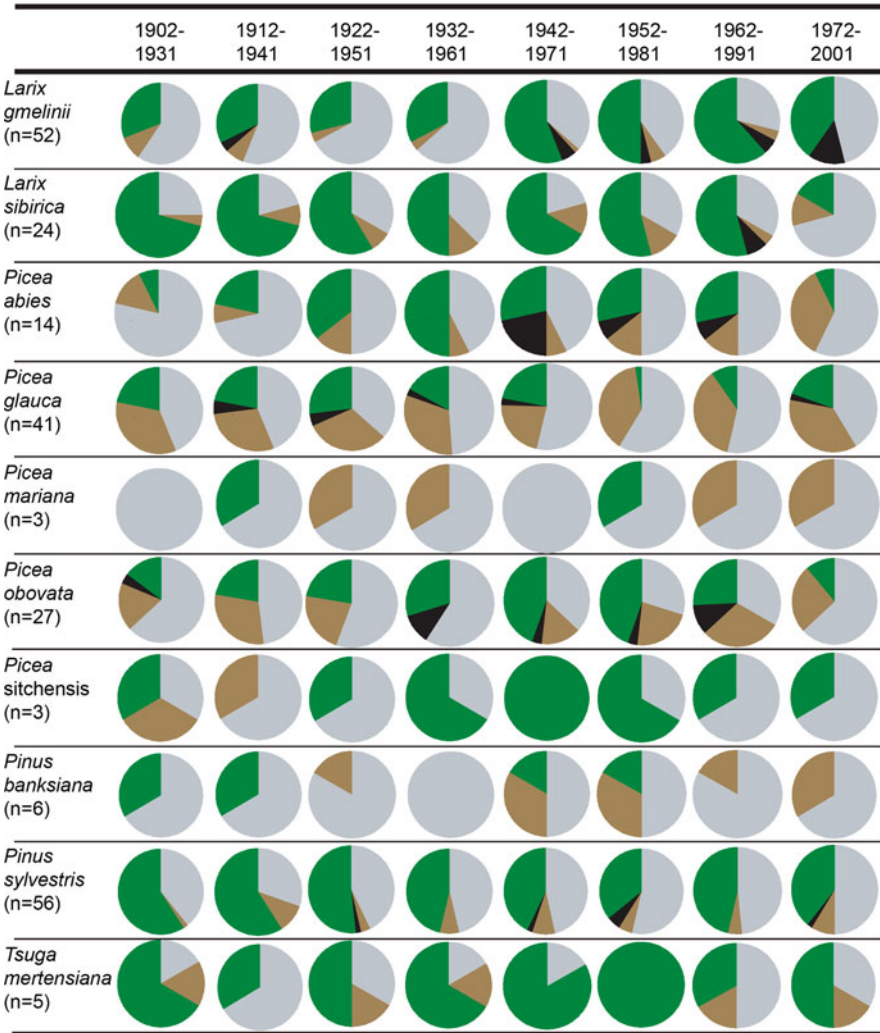
Fig. 2.7 Response to temperature of 10 boreal conifer species during eight 30-year time periods in the twentieth century. Each pie chart indicates the proportion of sites at which trees respond positively to warming (*green shading*), negatively to warming (*brown shading*), showed a mixed response to warming (positive correlations in some months, negative in others; *black shading*) or showed no response to warming (*grey shading*). Figure based on data from Lloyd and Bunn (2007)

Patterns of tree growth response to climate described in that study were idiosyncratic. Tree growth rates at many sites, particularly those occupied by the genus *Picea*, are declining in the presence of increasing temperatures (Fig. 2.7). This has been called the "divergence problem" and appears to be a widespread phenomenon in high latitude tree gowth (D'Arrigo et al. 2008). The explanation for declining

tree growth under conditions of longer and warmer growing seasons in the subarctic remains unknown, although a number of causes, including drought stress, pollution, global dimming (declining incident solar radiation), and direct temperature stress have been proposed. Although there is likely no single explanation for the phenomenon, the impact of drought on productivity (discussed earlier) is consistent with recent observations of reduced productivity in more densely forested areas. Focusing on the different responses of different species to warming may provide unique indications of change at specific locations or ecological regions. However, while tree ring data sets provide an integrative measure of growth for specific locations, they lack the complete spatial coverage afforded by productivity metrics like those derived from satellite observations. Combining these disparate data sets, therefore, would provide a useful approach to monitoring high latitude tree response to climate over large areas.

2.4.2 Correlation Between Satellite Vegetation Indices and Tree Rings

There is substantial co-variation between the tree-ring and satellite NDVI records, although defining the associations again seems to be species specific. An initial analysis shows that both spruce (*Picea* spp.) in Alaska and larch (*Larix* spp.) in Siberia are significantly positively correlated with July NDVI. Spruce growth correlated best with NDVI at a lag of 1 year, while larch, although not as strongly correlated with NDVI, had the highest correlation between current year growth and NDVI. This difference is very likely associated with the annual lifespan of needle production in larch compared with the long needle retention in spruce.

These initial correlations between tree growth from tree rings and NDVI suggest that it will be possible to merge the long records of growth from tree rings to the spatially contiguous records from satellites. There are, however, substantial challenges in determining causal links between canopy reflectance and cambial growth. The first is that the tree ring record, while extensive, is not systematically updated. In particular, the tree ring records from Russia mostly end in the mid 1990s and therefore have a smaller window that overlaps the satellite record. There are efforts underway to update these records, but the logistics for this are daunting. Given the species-specific responses seen in tree growth and climate (Fig. 2.7), it is critical that records be updated and well replicated.

Another issue affecting our ability to relate tree rings with NDVI data is that trees selected for dendroclimatic studies tend to be collected at the ecotone between forest and tundra or in sparse taiga. This causes problems when associating the relatively coarse NDVI data (8-km for the GIMMS data used here) to the individual tree ring sites. This scale mismatch is particularly problematic at latitudinal tree-line, in which much of the area within a satellite observation will primarily represent productivity of tundra rather than forest vegetation. One possible solution is to use the MODIS proportional tree cover (continuous fields) products to

weight the NDVI data proportionally by the amount of tree cover in a sampling window. This approach is being investigated by the co-authors (Beck, Bunn, Lloyd, and Goetz).

2.5 Simulation Model Projections of Arctic Vegetation Change

The observations described above demonstrate clear, albeit sometimes complex, associations between vegetation and climate variables. They also show changes in vegetation productivity that occurred across a broad geographic and ecological range of conditions in the past 20–25 years. In order to forecast how these changes will be expressed in the next few decades, however, ecosystem models are needed. In the following sections, we provide an overview of three different models that describe projected changes for different regions of the Arctic, and how these changes will vary between tundra and forest ecosystems. We first present a biome-scale model simulating broad changes across Northern Eurasia, and then describe and apply two models focused more specifically on smaller spatial domains and on the vegetation found in tundra versus the forest-tundra ecotones.

2.5.1 Changes in Distribution of Vegetation Types (BIOME4)

The BIOME4 global vegetation model has been designed to simulate patterns of land cover and the growth and decay of vegetation at relatively coarse resolution over large regions (e.g., Kaplan et al. 2002, 2003). The model is driven by basic climate and soils data and combines simplified representations of the biophysical and biochemical processes in ecosystems such as sunlight absorption by vegetation, photosynthesis, water uptake, and respiration, with ecological dynamics including establishment, succession, resource competition and migration. In order to simulate the great variety of vegetation types found globally, BIOME4 uses the concept of the Plant Functional Type (PFT). Each PFT represents a broad class of vegetation, including, e.g., temperate broadleaf deciduous trees, boreal evergreen needleleaf trees, or tropical herbaceous plants. Each PFT is defined by very broad ecoclimatic limits, and where PFT ranges overlap, they compete with each other in the model for light, water and nutrients. Vegetation models such as BIOME4 have been widely employed over the past years to explore the relationship between vegetation and climate and to make scenario calculations of the effects of future climate change on global and continental-scale land cover.

Starting with a data set of present-day observed climate (New et al. 2002) and soils (FAO 1995; Reynolds et al. 1999), we used the BIOME4 model to simulate potential natural vegetation distribution over Northern Eurasia at 10-km resolution (Fig. 2.8). Cool-temperate and cold boreal forests dominate the vegetation of eastern and Northern Eurasia, covering more than 15.6×10^6 km^2. The balance of the land cover of Northern Eurasia is occupied by a xerophytic shrublands and grasslands

at the southern boundary of boreal forest, and a sequence of tundra biomes, from high and low-shrub tundra at the polar treeline to cushion-forbs lichen and moss in the most extreme polar climate zones in the north. Biomes in Northern Eurasia are largely intact with little large-scale human impact except in the southern and westernmost boundaries of the region (see Chapter 3, this volume). Because the majority of Northern Eurasia is still occupied by potential natural vegetation, it may be particularly sensitive to future climate change and an important region for biophysical and biogeochemical feedbacks between the Earth surface and the atmosphere.

Using four future greenhouse gas emissions scenarios to run six Global Climate Models (GCMs), Kaplan and New (2006) prepared a series of future climate scenarios of the Earth under a 2°C global warming. The GCM simulations indicate that the Earth will have warmed by 2°C relative to preindustrial temperatures by 2026–2060, at which stage the area-mean annual temperature over the circumpolar Arctic (60–90°N) will have increased by 3.2–6.6°C. From the baseline land cover
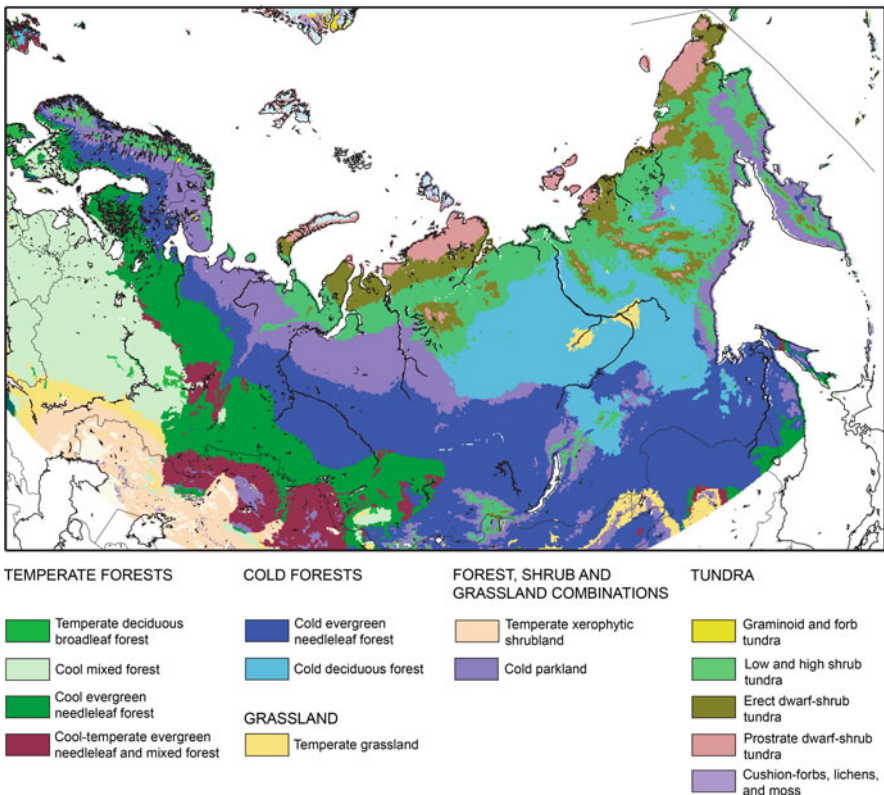

Fig. 2.8 Potential natural vegetation of the Northern Eurasia region at present-day predicted by the BIOME4 equilibrium global vegetation model (Kaplan et al. 2003), forced by late twentieth century mean CO_2 concentrations, climatology (New et al. 2002) and soils data (FAO 1995; Reynolds et al. 1999)
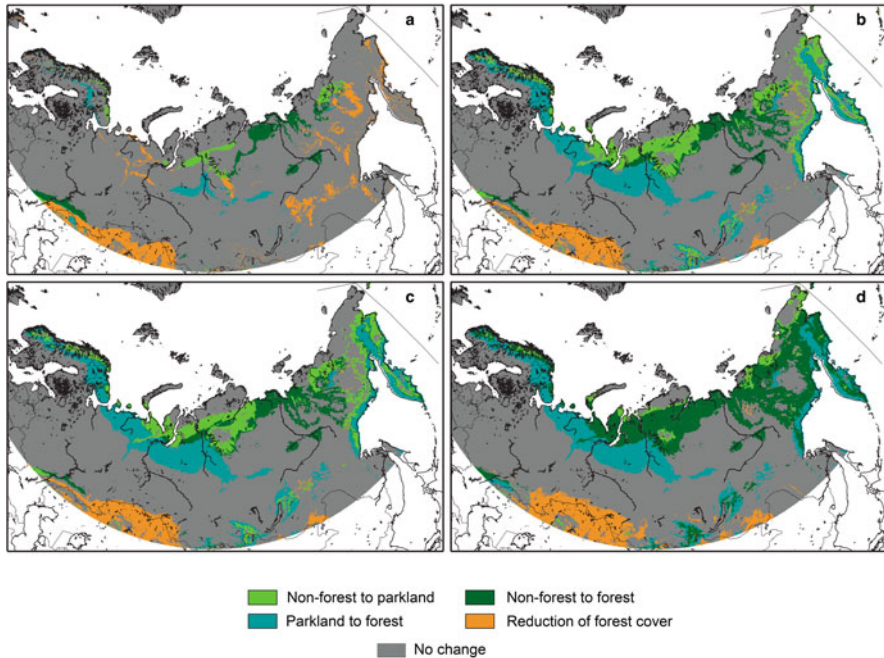
Fig. 2.9 Changes in vegetation cover relative to the potential natural state across the Northern Eurasia region predicted by BIOME4 in four scenarios of a future 2°C global warming: (**a**) 10th percentile "cool", (**b**) robust mean, (**c**) mean, and (**d**) 90th percentile "warm". For details of these climate change scenarios see Kaplan and New (2006)

illustrated in Fig. 2.8 and using these future climate scenarios, we simulated changes in the land cover of Northern Eurasia under a global 2°C warming. These future scenarios, illustrated in Fig. 2.9, indicate that forest extent could increase in Northern Eurasia on the order of 5×10^6 km^2 $\pm 1.8 \times 10^6$ (32%) with a corresponding 42% reduction in the tundra area. Tundra types generally shift north in the model simulations with the largest reductions in the extreme-cold tolerant dwarf-shrub tundra type, where nearly 60% of habitat is lost. Modeled shifts in the potential northern limit of trees reach up to 400 km from the present tree line, which may be limited by migration rates. Simulated physiological effects of the CO_2 increase (to ca. 475 ppm) at high latitudes were small compared with the effects of the change in climate. The increase in forest area of the Arctic could sequester 6 Pg of additional carbon, though this effect would be unlikely to be realized over next century (see Chapters 5 and 6, this volume).

The biophysical implications of these vegetation changes include increased absorption of solar radiation (decreasing albedo), which would have important feedbacks to the atmosphere, and changes in hydrological regimes because of increased snow retention (see Chapter 7, this volume). The increase in forest area in the Arctic would eventually be responsible for a large increase in carbon storage as tundra

soils are replaced by organic-rich forest soils, though this could be offset by the thawing and oxidation of organic loess (Yedoma) and peat that are currently locked in permafrost (Turetsky et al. 2007). The changes in Arctic vegetation simulated here would almost certainly have ramifications for biodiversity, effects on animal populations and human activities (Chapters 8 and 9, this volume).

2.5.2 Tundra Vegetation Dynamics (ArcVeg)

To simulate the dynamics of Northern Eurasian tundra, we used ArcVeg, a nutrient-based tundra vegetation model that projects the transient dynamics of arctic tundra plant communities (Epstein et al. 2000, 2001, 2007). ArcVeg uses a set of twelve tundra plant types including mosses, lichens, forbs, and several categories of graminoids and shrubs, and has been parameterized for the five arctic subzones described by Walker et al. (2005). Since plant-available nitrogen (N) can be strongly limiting for tundra plants (Chapin et al. 1995; Shaver and Chapin 1991), the model functions essentially by maintaining nitrogen mass balance, moving nitrogen among soil organic matter, plant-available nitrogen, and plant nitrogen pools. Plant parameters in the model include their nitrogen uptake efficiencies, biomass:N ratios, annual proportions of plant material senescing, probabilities of seedling establishment, and cold tolerances for growth. The model runs on an annual time step, however, the growing season is split into five distinct plant growth periods to capture the seasonality of vegetation growth across the full arctic climate gradient (i.e., Subzones A–E). The spatial resolution of the ArcVeg model is a 1×1 m grid cell, with the model simulating 100 stochastically different replicates of these grid cells (essentially a 10×10 m grid). The model has been validated using total and species-level biomass from field measurements throughout northern Alaska and Canada (Epstein et al. 2000, 2007). Model results and field data are relatively consistent both on the plant functional type level and for total biomass, indicating that the model is reasonable for making projections.

We simulated a 2°C warming in mean growing season temperatures, linearly ramped over a 50-year period for all five arctic subzones, which differ in their quantities of soil organic nitrogen, their rates of nitrogen mineralization, and their temperatures and growing season lengths. Model simulations were performed for 500 years in order for an equilibrium vegetation to develop, and then the model was run for an additional 500 years with the present climate. In Year 1000 a warming treatment was imposed, and the model was run for an additional 500 years (1,500 years total).

We again used the Yamal Peninsula in northwestern Siberia as the study region of interest. Due to a present lack of active layer Soil Organic Nitrogen (SON) field data from the Yamal region, we used Yamal soils data from an International Geosphere-Biosphere Programme (IGBP) global soil survey and projected active layer soil organic nitrogen using existing SON depth profiles from Alaska soils. We also assumed that for the Yamal region, reindeer would graze the tundra vegetation more frequently and intensely than the unmanaged caribou in North America.

These differences were reflected in our parameterization of the model. For the Yamal region, we assumed that Subzones C–E (southern High Arctic, and Low Arctic) are grazed more intensely than Subzones A and B (polar desert and northern High Arctic), which are off the mainland peninsula. For Subzones A and B we assumed that the system would be grazed every 10 years and that 25% of plant biomass was removed by grazing; for Subzones C, D and E, 50% of plant biomass was removed every 2 years.

In general, tundra in the Yamal region for all subzones responds to climate warming with increasing total biomass, especially for woody plants, and changes in plant community composition. For Subzones C, D and E in the Yamal region, there is less biomass compared to the same subzone in North America, due to heavy grazing by reindeer herds. Due to intense reindeer grazing and a preference for deciduous shrubs and lichens, Subzones D and E on the Yamal are dominated by evergreen shrubs and mosses.

For the Low Arctic tundra in Subzone E (Fig. 2.10a), warming led to an initial increase in dwarf-erect shrubs, and slight decreases in moss biomass due to competition with shrubs. Overall, the total biomass of Subzone E increased approximately 50% (400 g m^{-2}) dominated by the increase of evergreen shrubs (Fig. 2.10b). For Subzone D, warming increased the biomass of moss and evergreen shrubs (Fig. 2.10c). The total biomass of Subzone D also increased by approximately 50% (400 g m^{-2}, Fig. 2.10d).

For Subzone C, which is the southernmost subzone of the High Arctic, warming led to initial increases in mosses and an increase in evergreen shrubs. Total biomass of the Subzone C plant community increased by approximately 33%, (200 g m^{-2}) with warming over a period of about 50 years (Fig. 2.10f). For Subzone B, moss biomass increased substantially with warming, as did the biomass of shrubs (Fig. 2.10 g). Lichen biomass initially increased, but then dropped close to prior levels in Subzone B. Total biomass in Subzone B increased approximately 120% (600 g m^{-2}) in less than 100 years (Fig. 2.10 h). For Subzone A, the polar desert, moss and lichen biomass increased rapidly at first (Fig. 2.10i), however this was followed by increases in shrubs over a 150-year period. This increase in shrub biomass led to declines in both moss and lichen biomass, close to their original levels. Total biomass increased approximately 100% (200 g m^{-2}, Fig. 2.10j).

2.5.3 Tree-Line Dynamics (TreeMig)

Vegetation dynamics are influenced by both changing environmental conditions and anthropogenic land use. On a time scale of decades to centuries the increasing temperatures at northern high latitudes make it probable that vegetation will shift northward. Temperate species will be able to establish in regions currently too cold support them and, in the process, displace boreal species which, in turn, will migrate into tundra areas. Indications of early shifts of the arctic shrub- and tree-lines have already been observed across the arctic region, although not homogenously (Sturm
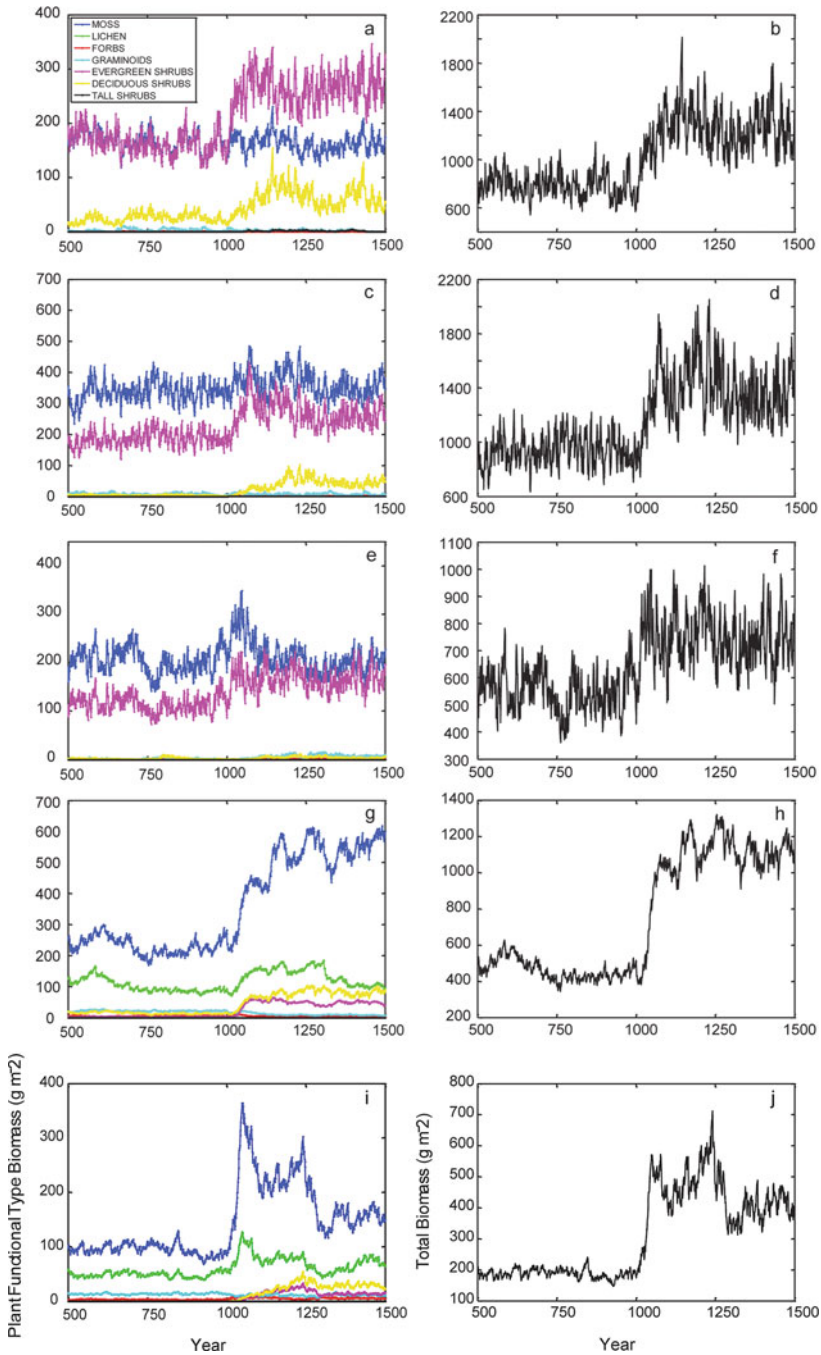
Fig. 2.10 Dynamics of above-ground biomass for seven plant functional types, and total biomass, as simulated by the ArcVeg model for arctic bioclimatic Subzones E **(a, b)**, D **(c, d)**, C **(e, f)**, B **(g, h)**, and A **(i, j)**. The model was run for each Subzone for 1,000 years with present climate, and then mean growing season temperatures were increased by 2°C, ramped linearly over a 50-year period

et al. 2001; Tape et al. 2006; Van Bogaert et al. 2007). The rate of this northward shift is bounded by the rate of climate change, i.e. the rate with which the species' fundamental niches will shift geographically. The ability of the species to migrate also limits the speed of these shifts.

Migration can be rather slow, because it involves a suite of dynamic population processes including seed production, seed dispersal, establishment, and maturation to seed production, i.e. to the next generation. In trees, maturation usually takes decades and can be prolonged by competition and adverse environmental conditions near niche limits. Thus, it is not realistic to assume an instantaneous presence of species at a location once the conditions become favorable, and assessing species' migration speed and associated shifts of their fundamental niches is not trivial.

The effects of climate change on biogeochemical cycling and species or plant functional type distributions have been examined with various coarse-scale biogeochemical models or dynamic global vegetation models. To get an impression of the order of magnitude of the lag due to migration processes, we studied the potential migration of boreal species into the tundra with a spatio-temporal dynamic forest model on an idealized transect through the boreal and tundra zone of Western Siberia. We focus on the temperature-driven population dynamics and spread of tree species, assuming other environmental factors were invariant.

We used the lattice-based, spatio-temporal dynamic tree species model TreeMig (Lischke et al. 2006). The model calculates local tree species population dynamics in each 1-km^2 grid cell, including seed bank dynamics, germination, growth, competition, mortality and seed production. The process functions depend on light and on climate variables (annual temperature sum, winter temperature, and drought). The species-specific parameters for the local dynamics had been determined previously in a study in the Ural region (unpublished). Within-cell heterogeneity is depicted by frequency distributions of tree density and consequently light intensity. Larger scale heterogeneity, e.g. a migration front within a cell, is not taken into account. Interactions between the cells occurs by seed dispersal, described by a dispersal kernel consisting of two negative exponentials, accounting for frequent short- and rare long-distance dispersal events. The mean dispersal distances (α) for species-specific wind-dispersed seeds have been estimated from sinking velocities and wind speed distributions (Lischke and Löffler 2006).

The simulation was run on a transect of 2,000 km length and 1 km width, ranging from latitude 61°N to 80°N. Climate data (monthly temperatures and monthly precipitation for 30 years) were interpolated between the latitudes from station data between longitude 74°E and 80°E along the eastern part of the Western Siberian lowlands. By adding a climate change scenario to the climate data, new means and standard deviations of yearly temperature sum, winter temperatures, and drought stress were calculated. The climate change scenario consisted of a spin-up phase of 600 years of current climate, followed by 100 years of linear temperature increase (2000–2100), according to the regional values of the A1B model mean from the Intergovernmental Panel on Climate Change (IPCC) 4th Assessment (Table 2.3, Christensen et al. 2007).

Table 2.3 Assumed temperature increases at year 2100, according to IPCC A1B scenario

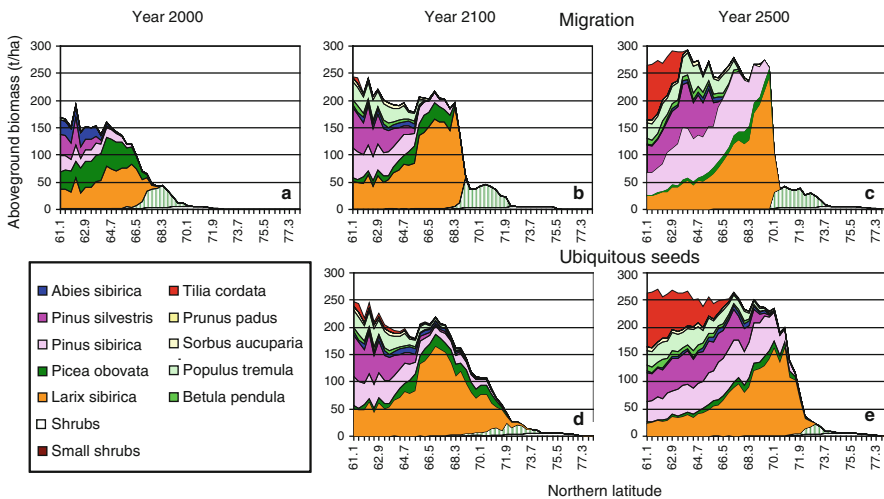| Months	Temperature increase
December, January, February	7°C
March, April, May	4.4°C
June, July, August	3.5°C
September, October, November	5.7°C

Fig. 2.11 Simulated above-ground biomass (tons per hectare) by species (y axis), with migration and seed dispersal. The x-axis is north latitude in decimal degrees

The model simulations were run in two modes: (i) seeds of all species were ubiquitously present, thus starting succession if the climatic conditions were appropriate, (ii) seeds reached a given cell only by dispersal, thus simulating migration.

In a first simulation under current conditions, we fine-tuned the species parameters for temperature dependence of growth and mortality such that the simulated tree line corresponds essentially to the position of the current observed tree line (Fig. 2.11a). Small shrubs and tundra vegetation as well as larger shrubs stretch from the tree line at about 67°N up to 72°N. Tree line is formed by larch and spruce, while other coniferous species are found more to the south. Under climate change, total above-ground biomass consistently increased (Fig. 2.11b–e), although larch and pine gained greater biomass at the expense of spruce. Broadleaf species appear in the southern part of the transect. If seeds are present, the shrubs and tree-line species reach their new range almost completely by 2100 (Fig. 2.11d), whereas within taiga, succession was finished by about 2300. With migration included (Fig. 2.11b, c), all shifts were delayed. At year 2100 none of the species has reached the same range as with seeds present, and even at year 2500, the tree species lag behind; only the shrub-line advanced to its new extent.
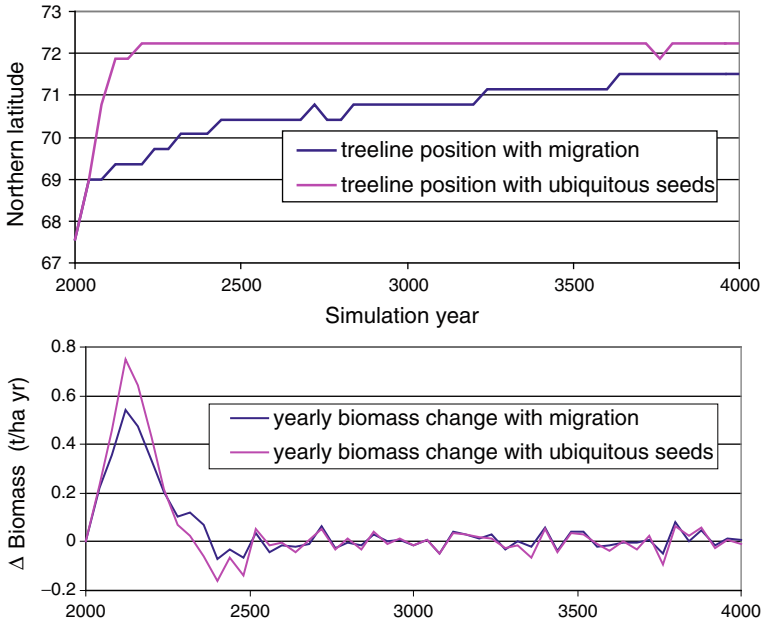
Fig. 2.12 (**a**) Simulated yearly tree-line position change (degrees north latitude) with migration and ubiquitous seeds. (**b**) Simulated yearly biomass change (tons per hectare per year) with migration and ubiquitous seeds

The comparison of tree-line position (defined as a 50 t/ha threshold) over the long term with and without ubiquitous seeds demonstrates the migrational lag of the latter case (Fig. 2.12). Even at year 4000 the tree-line of the migrating species has not yet reached the climatic distribution boundary. The rate of the tree-line shift decreased from an initial 2,000 to 150 m year^{-1} at the end of the simulation period, which corresponds well with migration speeds reconstructed from Holocene pollen data (Clark 1998). The average yearly biomass change on the transect shows the same characteristics for both modes: a strong biomass build-up from year 2000 to 2300, followed by a smaller biomass loss for about 200 years. With migration this pattern is less pronounced and delayed by about 50 years.

These simulations indicate that migration without ubiquitous seeds produces biome boundary changes much more slowly, resulting in lagged feedbacks to the climate system. For example, the treeless area is much larger for a longer period with migration than with ubiquitous seeds, potentially keeping albedo from declining. Biomass increase and associated carbon sequestration is also slower with migration included. The importance of simulating migration is supported by another similar study with two climate change scenarios and slightly different species parameters (Epstein et al. 2007). The current study agrees well in the duration of the lag and the rate of migration. The primary differences are in the representation of the shrub tundra and the nearly complete suppression of spruce after climate change.

The representation and simulations of vegetation dispersal and migration under climate change presented here are, however, limited. Many aspects of ecosystem dynamics have not been taken into account, including plant ecophysiology, soil dynamics, permafrost and its thawing, fires and their species-specific associations pest outbreaks, landscape heterogeneity, and the influences of human land use. Moreover, the model has uncertainties in the parameters relevant to dispersal and migration, e.g., wind-dispersed seeds can be uplifted to higher atmospheric layers and probably travel much farther than via near-surface winds (Nathan et al. 2002). Even more uncertain are the frequencies and distances of seed transport by animals. A thorough characterization of the spatio-temporal behavior of the model and adaptation of the parameters is required. Long-term spatial data on vegetation change are also needed. The best data source for testing simulations of long-term vegetation change is pollen assemblages. Model comparisons to pollen data are reliable only for long time periods and over broad areas. Finally, large-scale assessments of the influence of vegetation dynamics, and eventual coupling to climate models, implies computational challenges in better representing dispersal and migration speeds (Epstein et al. 2007).

2.6 Conclusions

Satellite imagery, and information derived from those observations, has become absolutely essential to monitoring remote areas across the Arctic, particularly given the extensive geographic scope and relatively few field measurements in this vast domain. The current satellite data record, particularly that from the AVHRR, is now of sufficient duration (30 years) to conduct meaningful analyses of inter-annual variability and trends in vegetation productivity. Further refinements in the observational data sets are needed, as are efforts to inter-calibrate sensor measurements with newer satellite platforms to ensure continuity of Earth observation data records. Nonetheless, the analyses summarized here demonstrate the utility of the satellite data for monitoring changes and trends through time, including the associations among vegetation productivity, surface temperature, and sea ice concentrations under different climate conditions.

Similarly, satellite studies of boreal forests above 60°N can be used for extending the growing tree ring database, despite the mixture of different cover types (tree versus tundra vegetation) within the satellite observations and the different responses of individual tree species to warmer temperatures. There are complementary approaches to analyzing these disparate data sets, and there is great potential for effectively extending the relatively short record from the satellites to the longer-term records of tree ring growth. Developing robust statistical models between the satellite and tree ring records also has the potential to refine process models of change in the northern high latitudes, including better estimates of the linked changes in radiation, meteorology, productivity and associated carbon exchange.

Finally, models of vegetation distribution, tree migration, and tundra vegetation responses to climate warming are currently able to capture logical transitions

and productivity changes consistent with expectations under a warming climate, but substantial refinements to the models are needed, particularly to capture dispersal mechanisms, migration rates, and changes in biogeochemical cycling (see Chapter 6, this volume). Continued collection and associated improvements to observations are also needed, not only to inform the models but also to calibrate and validate the outcomes of model simulations under the wide range of conditions that are predicted to occur across the arctic region in the next few decades. It is primarily through the combined use of field and satellite measurements that we will be able to capture the various feedbacks between terrestrial ecosystems and the physical climate system, and better predict how those changes will be expressed so that arctic communities and resource managers can plan and adapt to the inevitable changes that will follow.

References

Achard F, Eva HD, Mollicone D, Beuchle R (2008) The effect of climate anomalies and human ignition factor on wildfires in Russian boreal forests. Philos Trans R Soc Lond B. doi:10.1098/rstb.2007.2203

ACIA (2004) Impacts of a warming Arctic. In: Hassol SJ (ed) Arctic climate impact assessment overview report. Cambridge University Press, Cambridge, p 144

Angert A, Biraud S, Bonfils C, Henning CC, Buermann W, Pinzon J, Tucker CJ, Fung I (2005) Drier summers cancel out the CO2 uptake enhancement induced by warmer springs. Proc Natl Acad Sci USA. doi:10.1073/pnas.0501647102

Bala G, Caldeira K, Wickett M, Phillips TJ, Lobell DB, Delire C, Mirin A (2007) Combined climate and carbon-cycle effects of large-scale deforestation. Proc Natl Acad Sci USA. doi:10.1073/pnas.0608998104

Bhatt U, Walker D, Raynolds M, Comiso J (2008) Examining relationships between sea ice and Arctic vegetation on the Pan-Arctic regional and site scales. Eur Res Abst 10:EGU2008-A-11271

Bunn AG, Goetz SJ (2006) Trends in satellite observed circumpolar photosynthetic activity from 1982–2003: the influence of seasonality, cover type and vegetation density. Earth Interact 10:1–19

Bunn AG, Goetz SJ, Kimball JS, Zhang K (2007) Northern high latitude ecosystems respond to recent climate change. EOS 88:333–335

Chapin FS III, Bret-Harte MS, Hobbie SE, Zhong, H (1996) Plant functional types as predictors of transient responses of Arctic vegetation to global change. J Veg Sci 7:347–358

Chapin FS III, Callaghan TV, Bergeron Y, Fukuda M, Johnstone JF, Juday G, Zimov SA (2004) Global change and the boreal forest: thresholds, shifting States or gradual change? Ambio 33:361–365

Chapin FS III, Shaver GR, Giblin AE, Nadelhoffer KJ, Laundre JA (1995) Responses of Arctic Tundra to experimental and observed changes in climate. Ecology 76(3):694–711. doi:10.2307/1939337

Chapin FS III, Sturm M, Serreze MC, McFadden JP, Key JR, Lloyd AH, McGuire AD, Rupp TS, Lynch AH, Schimel JP, Beringer J, Chapman WL, Epstein HE, Euskirchen ES, Hinzman LD, Jia G, Ping CL, Tape KD, Thompson CDC, Walker DA, Welker JM (2005) Role of land-surface changes in Arctic summer warming. Science 310:657–660

Christensen JH, Hewitson B, Busuioc A, Chen A, Gao X, Held I, Jones R, Kolli RK, Kwon WT, Laprise R, Magaña Rueda V, Mearns L, Menéndez CG, Räisänen J, Rinke A, Sarr A, Whetton P (2007) Regional climate projections. In: Solomon S, Qin D, Manning M, Chen Z, Marquis M, Averyt KB, Tignor M, Miller HL (eds) Climate change 2007: the physical science

basis. Contribution of working group I to the 4th assessment report of the intergovernmental panel on climate change. Cambridge University Press, Cambridge

Clark J (1998) Why trees migrate so fast: confronting theory with dispersal biology and the paleorecord. Am Nat 152:204–224

Comiso JC (2002) A rapidly declining perennial sea ice cover in the Arctic. Geophys Res Lett 29(20):1956. doi:10.1029/2002GL015650

Comiso JC (2003) Warming trends in the Arctic from clear-sky satellite observations. J Clim 16:3498–3510

Comiso JC (2006) Arctic warming signals from satellite observations. Weather 61:70–76

Comiso JC, Nishio F (2008) Trends in the sea ice cover using enhanced and compatible AMSR-E,SSM/I, and SMMR data. J Geophys Res 113(C02S07). doi:10.1029/2007JC004257

D'Arrigo R, Wilson R, Lipert B, Cherubini P (2008) On the 'divergence problem' in northern forests: a review of the tree-ring evidence and possible causes. Glob Planet Change. doi:10.1016/j.physletb.2003.10.071

Deser C, Walsh JE, Timlin M (2000) Arctic sea ice variability in the context of recent atmospheric circulation trends. J Clim 13:617–633

Epstein HE, Calef MP, Walker MD, Chapin FS III, Starfield AM (2004) Detecting changes in arctic tundra plant communities in response to warming over decadal time scales. Glob Change Biol 10:1325–1334

Epstein HE, Chapin FS III, Walker MD, Starfield AM (2001) Analyzing the functional type concept in arctic plants using a dynamic vegetation model. Oikos 95:239–252

Epstein HE, Kaplan JO, Lischke H, Yu Q (2007) Simulating future changes in arctic tundra and sub-arctic vegetation. Comput Sci Eng 9:12–23

Epstein, HE, Walker MD, Chapin FS III, Starfield AM (2000) A transient, nutrient-based model of arctic plant community response to climatic warming. Ecol Appl 10:824–841

Field CB, Lobell DB, Peters HA, Chiariello NR (2007) Feedbacks of terrestrial ecosystems to climate change. Ann Rev Environ Resour 32:1–29

Food and Agriculture Organization (FAO) (1995) Digital soil map of the world and derived soil properties. Food and Agric Org, Rome

Forbes BC, Marc Macias F, Pentti Z (2010) Russian arctic warming and 'greening' are closely tracked by tundra shrub willows. Glob Change Biol 16(5):1542–1554

Forbes BC, Stammler F, Kumpula T, Meschtyb N, Pajunen A, Kaarlejrvi E (2009) High resilience in the Yamal-Nenets social, ecological system, West Siberian Arctic, Russia. Proc Natl Acad Sci 106(52):22041–22048

Friedl MA, McIver DK, Hodges JC, Zhang XY, Muchoney D, Strahler AH, Woodcock CE, Gopal S, Schneider A, Cooper A, Baccini A, Gao F, Schaaf C (2002) Global land cover mapping from MODIS: algorithms and early results. Remote Sens Environ 83:287–302

Goetz SJ, Bunn AG, Fiske GJ (2005) Satellite observed photosynthetic trends across boreal North America associated with climate and fire disturbance. Proc Natl Acad Sci USA. doi:10.1073/pnas.0506179102

Goetz SJ, Fiske G, Bunn A (2006) Using satellite time series data sets to analyze fire disturbance and recovery in the Canadian boreal forest. Rem Sens Environ 101:352–365

Goetz SJ, Mack MC, Gurney KR, Randerson JT, Houghton RA (2007) Ecosystem responses to recent climate change and fire disturbance at northern high latitudes: observations and model results contrasting Northern Eurasia and North America. Environ Res Lett 2(4). doi:10.1088/1748-9326/2/4/045031

Goetz SJ, Prince SD (1999) Modeling terrestrial carbon exchange and storage: evidence and implications of functional convergence in light use efficiency. Adv Ecol Res 28:57–92

Goulden ML, Wofsy SC, Harden JW, Trumbore SE, Crill PM, Gower ST, Fries T, Daube BC, Fan SM, Sutton DJ, Bazzaz A, Munger JW (1998) Sensitivity of boreal forest carbon balance to soil thaw. Science 279:214–216

Harrison SP, Prentice IC (2003) Climate and CO_2 controls on global vegetation distribution at the last glacial maximum: analysis based on paleovegetation data, biome modelling and palaeoclimate simulations. Glob Chang Biol 9:983–1004

Jia GJ, Epstein HE, Walker DA (2003) Greening of the Alaskan Arctic over the past two decades. Geophys Res Lett. doi:10.1029/2003GL018268

Jia GJ, Epstein HE, Walker DA (2004) Controls over intra-seasonal dynamics of AVHRR NDVI for the Arctic tundra in northern Alaska. Int J Rem Sens 25:1547–1564

Jia GJ, Epstein HE, Walker DA (2006) Spatial heterogeneity of tundra vegetation in response to recent temperature changes. Glob Change Biol 12:42–55

Kaplan JO, Bigelow NH, Prentice IC, Harrison SP, Bartlein PJ, Christensen TR, Cramer W, Matveyeva NV, McGuire AD, Murray DF, Razzhivin VY, Smith B, Walker DA, Anderson PM, Andreev AA, Brubaker LB, Edwards ME, Lozhkin AV (2003) Climate change and Arctic ecosystems: 2. Modeling, paleodata-model comparisons, and future projections. J Geophys Res 108(D19):8171. doi:10.1029/2002JD002559

Kaplan JO, New M (2006) Arctic climate change with a 2°C global warming: timing, climate patterns and vegetation change. Clim Change 79:213–241

Kaplan JO, Prentice IC, Buchmann N (2002) The stable carbon isotope composition of the terrestrial biosphere: modeling at scales from the leaf to the globe. Glob Biogeochem Cycles. doi:10.1029/2001GB001403

Kasischke ES, Stocks BJ (eds) (2000) Fire, climate change and carbon cycling in the boreal forest. Springer, New York

Kimball JS, McDonald KC, Zhao M (2006) Spring thaw and its effect on terrestrial vegetation productivity in the Western Arctic observed from satellite microwave and optical remote sensing. Earth Interact 10:1–22

Lischke H, Löffler T (2006) Intra-specific density dependence is required to maintain diversity in spatio-temporal forest simulations with reproduction. Ecol Model 198:341–361

Lischke H, Zimmermann NE, Bolliger J, Rickebusch S, Löffler TJ (2006) TreeMig: a forest-landscape model for simulating spatio-temporal patterns from stand to landscape scale. Ecol Model 199:409–420

Lloyd AH (2005) Ecological histories from Alaskan tree lines provide insight into future change. Ecology 86:1687–1695

Lloyd AH, Bunn AG (2007) Responses of the circumpolar boreal forest to 20th century climate variability. Environ Res Lett. doi:10.1088/1748-9326/2/4/045013

Mack M, Treseder K, Manies K, Harden J, Schuur E, Vogel J, Randerson J, Chapin FS (2008) Recovery of aboveground plant biomass and productivity after fire in mesic and dry black spruce forests of interior Alaska. Ecosystems 11(2):209–225

McGuire AD, Anderson LG, Christensen TR, Dallimore S, Guo L, Hayes DJ, Heimann M, Lorenson TD, Macdonald RW, Roulet N (2009) Sensitivity of the carbon cycle in the Arctic to climate change. Ecol Monogr 79:523–555

Myneni RB, Keeling CD, Nemani RR (1997) Increased plant growth in the northern high latitudes from 1981 to 1991. Nature 386:698–701

Nathan R, Katul GG, Horn HS, Thomas SM, Oren R, Avissar R, Pacala SW, Levin SA (2002) Mechanisms of long-distance dispersal of seeds by wind. Nature 418:409–413

Neigh CSR, Tucker CJ, Townshend JRG (2008) North American vegetation dynamics observed with multi-resolution satellite data. Rem Sens Environ 112:1749–1772

Nemani RR, Keeling CD, Hashimoto H, Jolly WM, Piper SC, Tucker CJ, Myneni RB, Running SW (2003) Climate-driven increases in global terrestrial net primary production from 1982 to 1999. Science 300:1560–1563. doi:10.1126/science.1082750

New M, Lister D, Hulme M, Makin I (2002) A high-resolution data set of surface climate over global land areas. Clim Res 21:1–25

Pavelsky TM, Smith LC (2004) Spatial and temporal patterns in Arctic river ice breakup observed with MODIS and AVHRR time series. Rem Sens Environ 93:328–338

Randerson JT, Liu H, Flanner MG, Chambers SD, Jin Y, Hess PG, Pfister G, Mack MC, Treseder KK, Welp LR, Chapin FS, Harden JW, Goulden ML, Lyons E, Neff JC, Schuur EAG, Zender CS (2006) The impact of boreal forest fire on climate warming. Science 314(5802):1130–1132. doi:10.1126/science.1132075

Raynolds MK (2009) Circumpolar Arctic NDVI and vegetation types: a spatial analysis of the distribution patterns and effects of climate and substrate. Ph.D Thesis, University of Alaska, Fairbanks.

Reynolds CA, Jackson TJ, Rawls WJ (1999) Estimating available water content by linking the FAO soil map of the World with global soil profile databases and pedo-transfer functions. AGU Spring Meeting, American Geophysical Union, Boston

Schuur EAG, Vogel JG, Crummer KG, Lee H, Sickman JO, Osterkamp TE (2009) The effect of permafrost thaw on old carbon release and net carbon exchange from tundra. Nature 459(7246):556–559

Serreze MC, Walsh JE, Chapin FS, Osterkamp T, Dyurgerov M, Romanovsky V, Oechel WC, J. Morison WC, Zhang T, Barry RG (2000) Observational evidence of recent change in the Northern high-latitude environment. Clim Change 46(1–2):159–207. doi:10.1023/A:1005504031923

Shaver GR, Chapin FS (1991) Production: biomass relationships and element cycling in contrasting arctic vegetation types. Ecol Monogr 61:1–31

Shaver GR, Street LE, Rastetter EB, van Wijk MT, Williams M (2007) Functional convergence in regulation of net CO_2 flux in heterogeneous tundra landscapes in Alaska and Sweden. J Ecol 95:802–817

Slayback DA, Pinzon JE, Los SO (2003) Northern hemisphere photosynthetic trends 1982–1999. Glob Change Biol 9:1–15

Soja AJ, Tchebakova NM, French NHF, Flannigan MD, Shugart HH, Stocks BJ, Sukhinin AI, Parfenova EI, Chapin FS III, Stackhouse PW Jr (2007) Climate-induced boreal forest change: preditions versus current observations. Glob Planet Change 56:274–296. doi:10.1016/J.GLOPLACHA.2006.07.028

Stroeve J, Markus T, Meier W, Miller J (2006) Recent changes in the Arctic melt season. Ann Glaciol 44:367–374

Sturm M, Racine C, Tape K (2001) Climate change: increasing shrub abundance in the Arctic. Nature 411:546–547

Tape K, Sturm M, Racine C (2006) The evidence for shrub expansion in Northern Alaska and the Pan-Arctic. Glob Change Biol 12:686–702

Treshnikov AF (1985) Atlas of the Arctic. Central Administrative Board of Geodesy and Cartography of the Ministereal Council of the USSR, Moscow (in Russian)

Turetsky MR, Wieder RK, Vitt DH, Evans RJ, Scott KD (2007) The disappearance of relict permafrost in boreal north America: effects on peatland carbon storage and fluxes. Glob Change Biol 13(9):1922–1934

Van Bogaert R, Walker D, Jia GJ, Grau O, Hallinger M, De Dapper M, Jonasson C, Callaghan TV (2007) Recent Changes in Vegetation. Arctic Report Card 2007. http://www.arctic.noaa.gov/reportcard/essay_vanbogaert.html. Accessed 1 June 2008

Walker DA, The CAVM Team (2005) The circumpolar arctic vegetation map. J Veg Sci 16:267–282

Walker MD, Wahren CH, Hollister RD, Henry GH, Ahlquist LE, Alatalo JM, Bret-Harte MS, Calef MP, Callaghan TV, Carroll AB, Epstein HE, Jónsdóttir IS, Klein JA, Magnússon B, Molau U, Oberbauer SF, Rewa SP, Robinson CH, Shaver GR, Suding KN, Thompson CC, Tolvanen A, Totland Ø, Turner PL, Tweedie CE, Webber PJ, Wookey PA (2006) Plant community responses to experimental warming across the tundra biome. Proc Natl Acad Sci USA. doi:10.1073/pnas.0503198103

Zhang K, Kimball JS, Hogg EH, Zhao M, Oechel WC, Cassano JJ, Running SW (2008) Satellite-based model detection of recent climate-driven changes in northern high-latitude vegetation productivity. J Geophys Res Biogeosci 113(G03033). doi:03010.01029/02007JG000621